Role of interfacial amino acid residues in assembly, stability, and conformation of a spherical virus capsid

Juan Reguera, Aura Carreira, Laura Riolobos, José María Almendral, and Mauricio G. Mateu*

Centro de Biología Molecular Severo Ochoa (CSIC–UAM), Universidad Autónoma de Madrid, Cantoblanco, 28049 Madrid, Spain

Edited by Alan Fersht, University of Cambridge, Cambridge, United Kingdom, and approved January 12, 2004 (received for review November 24, 2003)

Twenty-eight amino acid residues involved in most noncovalent interactions between trimeric protein subunits in the capsid of the parvovirus minute virus of mice were truncated individually to alanine, and the effects on capsid assembly, thermostability, and conformation were analyzed. Only seven side chains were essential for protein subunit recognition. These side chains virtually corresponded with those that either buried a large hydrophobic surface on trimer association or formed buried intertrimer hydrogen bonds or salt bridges. The seven residues are evolutionarily conserved, and they define regularly spaced spots on a thin equatorial belt surrounding each trimer. Truncation of the many side chains that were dispensable for assembly, including those participating in solvent-accessible polar interactions, did not substantially affect capsid thermostability either. However, the interfacial residues located at the base of the pores delineating the capsid five-fold axes participated in a heat-induced conformational rearrangement associated with externalization of the capsid protein N terminus, and they were needed for infectivity. Thus, at the subunit interfaces of this model virus capsid, only key residues involved in the strongest interactions are critical for assembly and stability, but additional residues fulfill other important biological roles.

Protein–protein recognition mediates many fundamental biological processes. A detailed knowledge of these processes requires the determination of the structural, energetic, and functional roles of individual amino acid residues and interactions in protein–protein interfaces. These studies have been generally undertaken by using small protein–ligand complexes or oligomeric proteins of moderate size (reviewed in ref. 1; see also refs. 2–4). In contrast, for multimeric protein complexes, such as viral capsids (5, 6) or large cellular assemblies, little is known about the specific molecular determinants of protein association and stability. Mutational studies of virus capsids, generally focused on a few specific amino acid residues, have provided important insights (7–22). However, exhaustive experimental studies on the relative importance of residues and molecular interactions in viral capsid assembly, disassembly, and/or stability are still very limited. These studies contribute also to the understanding of protein structure–function relationships and evolution under conflictive selective constraints (22–27), and they could be exploited possibly in the design of thermostable vaccines and antiviral agents promoting capsid disassembly or interfering with assembly (23, 28–31).

Many viruses, including viruses of medical or veterinary significance, have capsids of icosahedral symmetry. The icosahedral $T = 1$ capsids of parvoviruses (32–37) are formed by 60 protein subunits that are contributed by three nonidentical polypeptide chains (VP1, VP2, and VP3). These polypeptides derive, however, from a single gene and show identical fold and core sequence (Fig. 1). In the minute virus of mice (MVM) (35, 36), as in other parvoviruses, VP2 (the major capsid protein) is able to self-assemble into empty capsids, known as virus-like particles (VLPs) (38). VP1 includes the VP2 sequence plus a N-terminal extension (39). VP3 results from the cleavage of the N terminus of some VP2 subunits (40). Intersubunit contacts in the parvovirus capsid essentially involve residues and structural elements that are shared by all three proteins, and both the structure and physical properties, including thermostability, of parvovirus VLPs are very similar to those of natural capsids (32, 33, 36, 38, 41, 42).

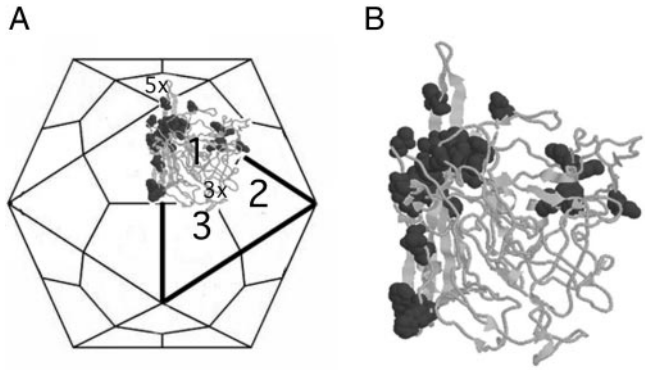

Fig. 1. (*A*) Schematic representation of the MVM capsid. Thick lines delimit 1 of the 20 identical trimeric subunits, and the three VP2 subunits within this trimer are numbered 1, 2, and 3. A ribbon model of the structure of one VP2 subunit has been superimposed. (*B*) Detail of the VP2 capsid subunit. For this subunit, the 28 residues located at the intertrimer interfaces and chosen for mutation are shown as space-filling models.

Several lines of evidence indicate that trimers of the capsid protein (Fig. 1) are intermediates in the assembly of MVM and other parvoviruses. (*i*) The number of intersubunit contacts within trimers is much higher than it is between trimers (33, 43); (*ii*) transport of VP2 of MVM to the cell nucleus may require the formation of trimeric intermediates (44, 45); (*iii*) small amounts of trimers were detected in cells expressing canine parvovirus (CPV) proteins (42); and (*iv*) the presence of trimeric intermediates has been observed directly in cross-linking and sedimentation assays of a few MVM capsid mutants whose assembly was impaired by steric mutations at the intertrimer interfaces (L.R., J.R., M.G.M., and J.M.A., unpublished data). We have used the empty capsid of MVM for identifying at the intertrimer interfaces the molecular determinants of assembly and stability of the parvoviral capsid, one of the simplest models available for a spherical virus capsid or multimeric protein complex. The results reveal that only a few residues involved in intertrimer interactions have a critical role in assembly and stability. However, other interfacial residues are involved in a functionally important conformational change. The structural and biological implications of these findings are discussed.

Materials and Methods

Recombinant Plasmids and Mutagenesis. Site-directed mutagenesis of the VP2 gene of MVM strain p (MVMp) was carried out by

This paper was submitted directly (Track II) to the PNAS office.

Abbreviations: MVM, minute virus of mice; MVMp, MVM strain p; MVMi, MVM strain i; VLP, virus-like particle; T_m, transition temperature.

*To whom correspondence should be addressed. E-mail: mgarcia@cbm.uam.es.

www.pnas.org/cgi/doi/10.1073/pnas.0307748101

using the QuikChange system (Stratagene) on recombinant plasmids pSVtk-VP1/2 [which included the VP1/VP2 gene of MVMp and was derived from a molecular clone of the MVMp genome (46)] and pFB1-VP2 (47). The mutations were confirmed by automated sequencing. For expression in insect cells, the Bac-to-Bac baculovirus expression system (Invitrogen) and mutant pFB1-VP2 (as donor plasmids) were used to construct BM-VP2 baculovirus shuttle vectors containing the VP2 mutations. Introduction of mutations in the MVM infectious clone pMM984, originally provided by P. Tattersall (Yale University, New Haven, CT; ref. 48) and modified to include the VP2 sequence of MVMp, was carried out by subcloning.

Expression of VLPs. Recombinant bacmids BM-VP2 (parental and mutants) were used to transfect H5 insect cells essentially as described (47). The sequences of six mutant VP2 genes (*R83A*, *T249A*, *F55A*, *D507A*, *L537A*, and *S550A*) in the recombinant baculovirus DNA obtained were totally or partially determined as a final validation of the procedure. The infected cells were incubated until complete cytopathic effect, and they were then harvested. The cells were resuspended in lysis buffer (50 mM Tris·HCl, pH 8/150 mM NaCl/0.2% Triton X-100/0.2 mM EDTA/0.4 mM 4-(2-aminoethyl)benzenesulfonyl fluoride/26 μM bestatin/2.8 μM E64/0.2 μM leupeptin/0.06 μM aprotinin) and frozen at −70°C.

Purification and Sedimentation Analysis of Empty Capsids. A procedure described in refs. 38 and 47 was followed. The capsid preparations were found by SDS/PAGE and UV spectrophotometry to be essentially free of contaminants. The capsid (monomer) concentration was determined by using an extinction coefficient at 280 nm of $\varepsilon_{280} = 114{,}160\ M^{-1}\cdot cm^{-1}$. For mutants with a substituted tryptophan or tyrosine, the appropriate corrections were introduced.

Electroporation of Mammalian Cells, Infectivity Assays, and Immunofluorescence Assays. Procedures described in refs. 44 and 45 were followed. Briefly, NB324K cells were electroporated with plasmid pSVtk-VP1/VP2 or pMM984, carrying the appropriate mutations. Virions were recovered at 72 h from pMM984-transfected monolayers and titrated in standard plaque assays. Immunofluorescence assays were performed as described (44, 45), with minor modifications.

Spectrofluorimetry of MVM Capsids. A Cary Eclipse luminescence spectrophotometer (Varian) was used. Purified MVM capsids at a (monomer) protein concentration of 0.48 μM in PBS were added to a 2 × 10-mm cell and irradiated with UV light (excitation wavelength 295 nm). Temperature was increased continuously from 25°C to 85°C at a rate of 1°C per min, and the intrinsic tryptophan fluorescence at an emission wavelength of 330 nm was determined at 1-min intervals. The fluorescence changes were fitted to sigmoidal cooperative transitions by using the KALEIDAGRAPH (Abelbeck Software, Reading, PA), which allowed the precise determination of the half-transition temperature (T_m) (47). For analyses at acidic pH, a 0.96 μM solution of the capsid in PBS was diluted 1:1 with 50 mM phosphoric acid/sodium phosphate buffer (pH 2), and the final pH was determined. Measurements were normally started immediately after acidification, but the T_m was not affected, even after 40 min.

Molecular Graphics and Structural Analyses. An O_2 workstation (Silicon Graphics, Mountain View, CA), the PDB coordinates of MVM strain i (MVMi) (1MVM) (35, 36), and the programs INSIGHTII (Biosym Technologies, San Diego), RASMOL (49), and WHATIF (50) were used.

Results

Analysis of Intertrimeric Interactions and Selection of Interfacial Residues for Mutagenesis. We have inspected the noncovalent contacts between trimeric subassemblies in the crystallographic structure of the MVMi virion (35, 36). Within the imposed limits (cutoff distance 0.5 Å higher than the sum of the van der Waals radii of the two atoms considered), a total of 104 residues of the 587 amino acids per capsid monomer (VP2) were found to be involved in intertrimeric atomic contacts in MVM. The 38 N-terminal residues of VP2 were disordered in the crystal, suggesting that this segment, which may be externalized through the capsid five-fold axis (36), makes few or no stable contacts with other capsid residues. The side chains (beyond Cβ) of 80 residues per monomer are involved in intertrimer contacts, and they define the interfaces accessible to alanine mutation. Of these side chains, 30 have an essentially nonpolar nature and participate in van der Waals interactions only. However, only seven of these side chains and the aromatic ring of Y522 make extensive hydrophobic contacts between trimers. The 50 remaining interfacial side chains are polar and participate in van der Waals contacts, and 20 of them participate also in a total of 28 intertrimeric hydrogen bonds and four strict salt bridges (cutoff distance 3.5 Å). One of the charged residues at the contact interface and three additional charged residues may be involved in four medium-range electrostatic interactions (cutoff distances 3.5–5.5 Å). Longer-range interactions were not considered. In summary, both the hydrophobic effect and hydrogen bonding between a fair number of interfacial side chains could potentially make major contributions toward holding the trimeric subassemblies together. However, because of its 60-fold multiplicity, the loss of even a weak interaction could potentially have a significant negative effect on capsid stability (51). VP2 from the MVMp strain used in this work differed from that of MVMi in only 2.4% of its amino acid residues, and all but 1 (V551) of the 14 nonconserved residues were located away from the intertrimer interfaces. Thus, the intertrimer contacts are nearly identical in both MVM strains.

Based on all of the observations described above, 28 of the 79 interfacial amino acids whose side chains beyond Cβ are involved in intertrimer interactions within the MVMp capsid were chosen for mutagenesis (Table 1 and Fig. 1). The selected residues constituted a representative sample that accounted for 34% of the side chains at the interfaces between trimers. Because mutation of only one residue of any one pair involved in an intertrimer interaction would be enough to eliminate that interaction, truncation of the side chains of the selected residues to alanine would together disrupt a very high proportion of the intertrimer interactions, including all but two of the hydrogen bonds that involved side chains, all salt bridges and medium range charge–charge interactions, and nearly all major clusters of hydrophobic contacts. VP2 single variants in which the 28 selected residues were mutated individually to alanine were constructed and analyzed experimentally for empty-capsid assembly and stability.

Effect of Mutation of Interfacial Amino Acid Residues on Capsid Assembly. Individual truncation to alanine of all but one of seven apolar (V40, I84, I167, I207, W386, F526, and L537) and two polar (T249 and T569) side chains involved in a limited number of intertrimer van der Waals interactions (one to seven contacts) did not prevent high-level expression of VP2 in insect cells and assembly of mutant VLPs (Table 1). The only exception was the mutant T249A (see below). Truncation of eight polar side chains (S43, H72, N74, R83, N149, N170, D263, and S550) that were involved in one or two hydrogen bonds and between two and eight van der Waals contacts each did not prevent high-level expression of VP2 and VLP assembly either (Table 1). The same

Table 1. Effect of truncation of interfacial side chains on capsid assembly and stability

Capsid protein mutant	Group	Intertrimer interactions: Charge–charge interactions	Intertrimer interactions: Hydrogen bonds	Intertrimer interactions: van der Waals contacts	Conservation	T_M, °C
W543A	I	—	—	17 (15)	C	No assembly
W203A	I	—	—	12 (10)	C	No assembly
F247A	I	—	—	10 (9)	C	No assembly
F55A	I	—	—	12 (10)	—	73.3 (58.2)
Y522A	I, II	—	1 mc L505	19 (10)	C	No assembly
Q129A	II	—	2 mc V546	16 (3)	C	No assembly
K153A	III	D171	1 sc D171, 1 sc N504	6 (1)	C	No assembly
L537A	IV	—	—	7 (7)	—	74.1
F526A*	IV	—	—	6 (5)	—	74.5
W386A	IV	—	—	6 (2)	—	74.3 (56.9)
V40A*	IV	—	—	4 (2)	—	74.9 (58.9)
I207A	IV	—	—	1 (1)	—	72.5 (56.9)
I84A	IV	—	—	1 (0)	—	73.2 (54.6)
I167A	IV	—	—	1 (0)	—	72.4
N554A	IV	—	—	10 (4)	—	75.5
T249A	IV	—	—	2 (2)	C	No assembly
T569A	IV	—	—	2 (1)	—	73.9
R83A	V	—	2 mc P566	2 (0)	—	71.2
N149A*	V	—	2 sc R260	4 (1)	C	74.7 (59.9)
S550A	V	—	2 mc Q548	8 (0)	—	75.1
S43A*	V	—	1 mc L258	2 (0)	C	74.8 (59.2)
H72A	V	—	1 mc T506	8 (5)	C	73.4 (59.3)
N74A	V	—	1 mc D507	2 (0)	—	75.1
N170A*	V	—	1 sc D171	5 (0)	C	75.4 (59.4)
D263A*	V	—	1 mc S43	3 (0)	C	75.1 (59.7)
D507A	VI	K166	1 sc K166	3 (1)	—	74.0 (59.2)
K204A	VII	E79	1 sc N80, 1 mc E79	1 (0)	—	75.0
K241A	VII	D553	—	0 (0)	—	73.2

Mutations in the capsid protein have been included in groups I–VII according to the type of intertrimer interactions in which the truncated side chain is involved. I, multiple hydrophobic contacts; II, buried hydrogen bonds; III, buried salt bridges; IV, few hydrophobic contacts; V, surface hydrogen bonds; VI, surface salt bridges; VII, medium-range charge–charge interactions. The specific intertrimer interactions that would be disrupted by truncation to alanine of the specified residue are also listed. For van der Waals interactions, the total number of contacts are given, and the carbon–carbon contacts are given in parentheses. The transition temperature (T_M) for the capsid dissociation step is given at pH 7 and 2.7 (in parentheses). T_M for the wild-type capsid was 74.7 ± 0.5 at pH 7 and 58.6 ± 0.5) at pH 2.7 (mean ± SD of several independent experiments with different capsid preparations). For any given mutant, the fitting error was <0.5°C. mc, main chain; sc, side chain; C, conserved [in seven parvoviruses closely related to MVM (see ref. 43)].
*These mutations prevented the capsid conformational change from occurring.

lack of effect was observed when three solvent-exposed charge–charge interactions (one salt bridge and two medium-range interactions) were disrupted individually by mutations D507A, K204A, and K241A (Table 1). All of the above mutant VLPs could be purified to relatively comparable yields. In sharp contrast, single truncations to alanine of four of five side chains (F55, W203, F247, W543, and Y522) that were each involved in many 9-to-15 intertrimer hydrophobic contacts (Y522 was additionally involved in one hydrogen bond buried at the interface) prevented the accumulation of VP2 in insect cells (Table 1). Truncation of the polar side chains of Q129 (involved in two hydrogen bonds deeply buried at the trimer interfaces and in 16 additional van der Waals contacts) and K153 (involved in one salt bridge and one additional hydrogen bond buried at the interface and in six other van der Waals contacts) had an equally drastic effect (Table 1).

Failure of some mutant VP2 to accumulate in insect cells was probably a consequence of their inability to assemble into capsids, the synthesized monomer or the nonproductive intermediates formed being degraded by insect cell proteases. To show that these mutants were indeed unable to assemble into capsids, they were tested for capsid subunit expression and empty capsid assembly in mammalian cells. Expression of capsid proteins was detected by reactivity with a polyclonal Ab that recognizes epitopes in isolated VP2. Assembled capsids were detected by reactivity with an mAb that recognizes a capsid-specific, discontinuous epitope located at the vertex of the 3-fold spikes (52), far away from the intertrimer interfaces and from the residues mutated in this work. In mammalian cells, all tested mutant capsid proteins were expressed and accumulated to relatively high levels, as observed in immunofluorescence assays (Fig. 2 and data not shown). Both wild type and control mutants that formed VLPs in insect cells (e.g., L537A, F526A, and F55A) also assembled into empty capsids in mammalian cells. In contrast, none of the mutants that failed to accumulate in insect cells reacted with the anticapsid mAb in fluorescence assays and were, thus, defective in assembly (Fig. 2 and Table 1).

In summary, only 7 of 28 of the tested interfacial side chains per VP2 subunit were found to be involved critically in capsid assembly (Fig. 3). All seven residues were conserved and, except for T249, participated in the largest number of hydrophobic contacts between trimeric subunits or in buried intertrimer hydrogen bonds or salt bridges. T249 was involved in only a few intertrimer van der Waals contacts, but it formed part of a cluster

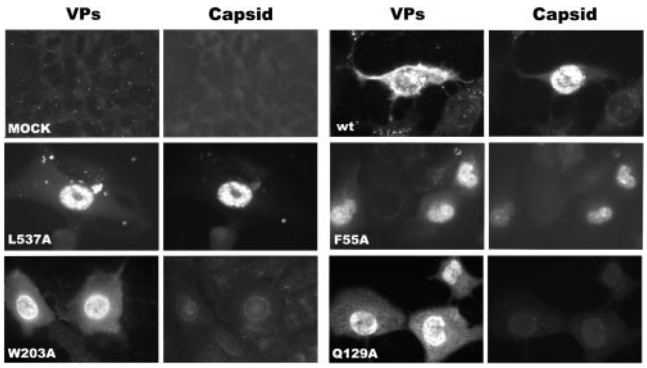

Fig. 2. Immunofluorescence detection of capsid proteins (VPs) and assembled capsids (Capsid) of MVM wild type (wt) and some representative mutants in transformed mammalian cells. Mock, mock-transformed cells.

of critical residues, which included F247 from the same subunit, W543 from a neighboring subunit in the same trimer, and W543 from a subunit in the neighboring trimer.

Effect of Interfacial Mutations on the Stability of the Assembled Capsid. Although disruption of most intertrimer interactions did not prevent capsid assembly, the capsids formed could still be destabilized because of the interactions lost. To test this possibility, the assembled nonmutated and mutant VLPs were purified. The electrophoretic mobility of VP2 and the sedimentation coefficient of the mutant capsid were not altered significantly in any case relative to the wild-type capsid (data not shown). Thus, all of the assembled mutant capsids were of the correct size. The capsid of MVMp contains 15 essentially buried tryptophans per

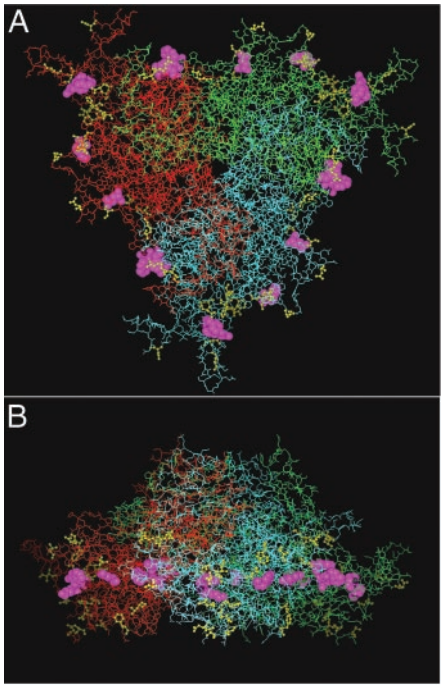

Fig. 3. Wireframe model of the structure of a trimeric assembly in the MVM capsid. (*A*) Frontal view. (*B*) Lateral view. In each VP2 subunit in the trimer (shown in different colors), the seven residues at the intertrimer interface whose side chains were found to be critical for assembly are represented as violet space-filling models. The 21 residues whose side chains were found not to be critical for assembly or stability are shown as yellow ball-and-stick models.

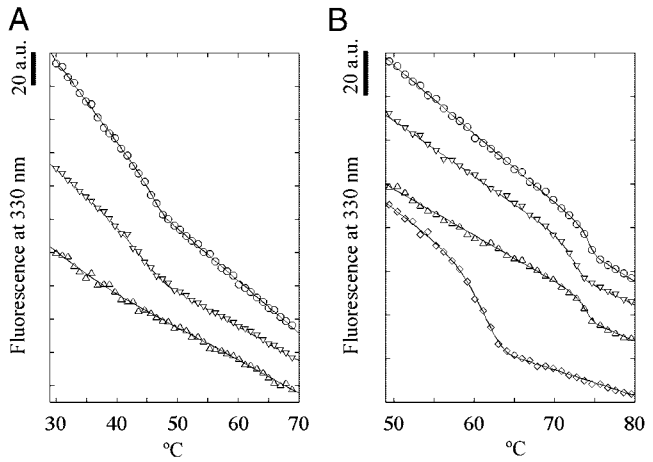

Fig. 4. (*A*) Conformational rearrangement of the MVM capsid at moderate temperatures. Open circles, wild type; inverted triangles, mutant S550A; and upright triangles, mutant V40A. (*B*) Dissociation of the MVM capsid at high temperatures. Open circles, wild type; inverted triangles, mutant H72A; upright triangles, mutant N149A at neutral pH; and diamonds, wild type at pH 2.7. In *A* and *B*, the curves were obtained in tryptophan emission fluorescence experiments and have been fitted to sigmoidal cooperative transitions and offset for clarity. The negative slope of the baselines corresponds to thermal quenching. a.u., arbitrary units.

monomer, and a few of them are located at the intertrimer interfaces. Thus, capsid dissociation could be probed by exposing the capsid to a controlled thermal gradient and following the change in intrinsic tryptophan fluorescence as a measurement of changes in tryptophan exposure to solvent (Fig. 4). The fluorescence curve obtained for the parental (nonmutated) MVM capsid revealed two clearly separated sigmoidal transitions. These have been shown (47) to respectively correspond to (*i*) a reversible conformational change (without capsid dissociation) that occurred with a T_m of 46°C (Fig. 4*A*), involved a change in the exposure of some capsid tryptophans to solvent, and involved also the externalization of the VP2 N terminus, as detected by the trypsin sensitivity of the exposed peptide segment; and (*ii*) the irreversible dissociation of the capsid with a T_m of 75°C (Fig. 4*B*), followed by capsid subunit denaturation. This step has been characterized further by changes in capsid hemagglutination activity and electrophoretic mobility, as well as by differential scanning calorimetry analyses. In a physiological buffer, the dissociation and denaturation of the capsid proceeded through an intermediate, which was apparently destabilized by the presence of a low concentration of guanidinium chloride, resulting in a two-state dissociation and denaturation transition. Chemical dissociation, followed by fluorescence spectroscopy, circular-dichroism spectroscopy, and molecular-size determinations, indicated that the dissociation and denaturation product obtained corresponded to a molten-globule-like monomeric state of the capsid protein (47). The specific dissociation T_m value obtained by fluorescence, which could be determined very precisely, has been used here as an indicator of the relative kinetic stability against dissociation of the mutant capsids with side-chain truncations at the intertrimer interfaces (Fig. 4*B*).

Acidification to pH 2.7 severely reduced capsid stability, as reflected in its T_m of dissociation (16°C below that obtained at neutral pH). In contrast, the 21 single interfacial mutations tested yielded, at pH 7 and 2.7, a T_m of dissociation indistinguishable, or only slightly reduced, from that of the nonmutated capsid at the same pH (Fig. 4*B* and Table 1). In brief, 21 of the 28 tested interfacial mutants per protomer assembled into capsids that were indistinguishable from the nonmutated native

BIOCHEMISTRY

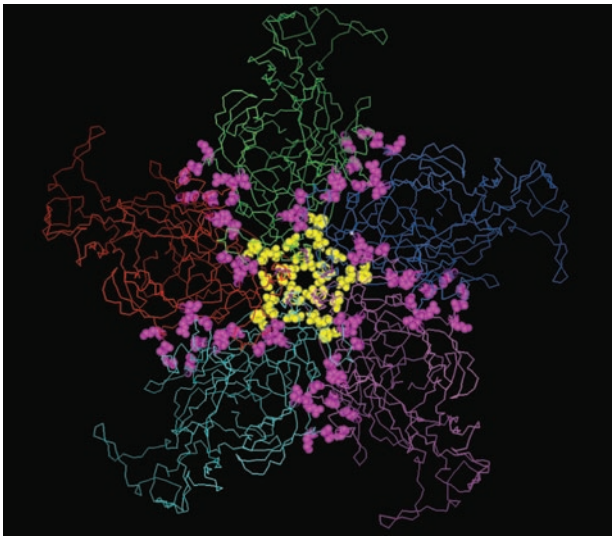

Fig. 5. Backbone model of the structure of five symmetry-related VP2 (shown in different colors) belonging to different trimers around the capsid pore at one of the capsid five-fold axes (center region). Mutated residues at the intertrimer interfaces are represented as space-filling models (except Ile-167, which is shown as a ball-and-stick model). The residues whose side chains were found to be involved in a heat-induced conformational change and externalization of the VP2 N termini are shown in yellow. The residues whose side chains could be truncated without abolishing the conformational rearrangement are shown in violet.

capsid in hydrodynamic behavior and had a similar stability against heat-induced dissociation.

Effect of Mutation of Interfacial Residues on a Capsid Conformational Transition That Exposes the VP2 N Terminus. In MVM virions, but not empty capsids, the N terminus of some VP2 molecules is exposed at the capsid surface (41). Exposure of this segment in empty capsids can be achieved *in vitro* by heat treatment (38), and there is structural evidence that externalization may occur through the pores located at the five-fold axes of the parvovirus capsid (32, 36). The transition temperature for exposure of the VP2 N termini was coincident, within error, with that of the conformational rearrangement detected by fluorescence (ref. 47 and see above). Most of the mutant capsids tested here showed this conformational rearrangement also, and the corresponding T_m did not differ significantly from that of the nonmutated capsid. However, six of the interfacial mutations prevented this transition from occurring (Fig. 4*A* and Table 1). Two of these six mutants (V40A and D263A), one mutant that preserved the conformational transition (I207A) and the nonmutated control, were also assayed directly for exposure of the VP2 N terminus on heating by using a protease-sensitivity assay. As expected, externalization of the N terminus was impaired, to some extent, in the mutants that showed no conformational transition in fluorescence assays (data not shown). Inspection of the MVM capsid structure (Fig. 5) revealed that, without exception, the five symmetry-related copies of every residue whose truncation abolished this conformational change formed the internal base of the pores located at the five-fold axes in the capsids of MVM and other parvoviruses. In sharp contrast, all of the mutations that did not abolish that transition, except I167A, were located far away from the five-fold axes. I167 was also not located at the base of the pore, but closer to the top on the capsid surface (Fig. 5).

Five of the six mutations at the intertrimer interfaces that prevented the transition from occurring, and 9 of the 15 mutations that did not, were introduced into an infectious MVMp clone. Wild type and mutants were tested for capsid protein expression and capsid assembly in mammalian cells by *in situ* immunofluorescence and for the formation of infectious progeny virus by plaque-formation assays (Table 2). All mutants and the wild type yielded similar amounts of capsid protein. Of the nine mutants that preserved the conformational change, only three (F55A, H72A, and R83A) yielded extremely low or undetectable viral titers. This effect was related to some defect in virion assembly or stability because these three mutants yielded few or no capsids on transfection (Table 2). These mutants produced normal amounts of empty capsids on transformation with the capsid proteins alone, suggesting some interference of nonstructural proteins or the viral DNA in the assembly of these mutant virions. The six other mutants that preserved the conformational transition formed normal amounts of capsids and yielded virus titers similar to wild type, or only moderately reduced (Table 2). Five of these six residues were not conserved among parvoviruses closely related to MVM (43). In sharp contrast, all five mutants that underwent no conformational alteration on mild heating (mutants with substitutions close to the five-fold axes pores) yielded extremely reduced viral titers or were noninfectious, despite all of them being able to form normal amounts of capsids. Four of these six residues (residues involved in intertrimer hydrogen bonds) were conserved among related parvoviruses (Table 1). To summarize these results, residues that surround the base of the pores at the five-fold axes are involved in a conformational rearrangement of the capsid and externalization of the VP2 N terminus. These residues are needed for completion of the viral cycle, despite being noncritical for capsid assembly and stability.

Table 2. Infectivity of MVM mutated at interfacial residues

Virus	Heat-induced rearrangement*	Capsid protein expression†	Capsid assembly in infected cells‡	Normalized virus titer**
Wild-type	Yes	++	++	1
F55A	Yes	++	−	$<8 \times 10^{-6}$
H72A	Yes	++	−	$<8 \times 10^{-7}$
R83A	Yes	++	+/−	$<5 \times 10^{-6}$
N74A	Yes	++	++	0.93
I84A	Yes	++	++	0.08
I167A	Yes	++	++	0.07
K204A	Yes	++	++	1.05
I207A	Yes	++	++	0.11
K241A	Yes	++	++	0.93
V40A	No	++	++	1.2×10^{-4}
S43A	No	++	++	$<4 \times 10^{-5}$
N149A	No	++	++	$<8 \times 10^{-7}$
N170A	No	++	++	$<5 \times 10^{-6}$
D263A	No	++	++	$<8 \times 10^{-6}$

++, signal comparable with wild type; +/−, positive but very weak signal; −, signal indistinguishable from the background.
*Determined by intrinsic tryptophan fluorescence of the capsid.
†Determined by intracellular inmunofluorescence assays with an anti-VP2 Ab.
‡Determined by intracellular immunofluorescence assays with an anticapsid Ab.
**Determined in plaque-formation assays. For normalization, the average absolute titer was divided by the average titer obtained for the wild-type virus in the same experiment. For any given mutant, except K241A and V40A, the weighted average of two experiments is indicated. SD within an experiment were ≈10% of the average titer. Titers obtained in different experiments generally differed by 5–10%.

Discussion

Structure–function analysis by alanine-scanning mutagenesis of the interfaces between the trimeric subassemblies in the icosahedral MVM capsid indicates that only a very small number of the interfacial side chains are critically needed for productive

oligomerization and capsid assembly. These few residues are conserved and either show the largest number of hydrophobic contacts between trimeric subunits or participate in deeply buried intertrimer hydrogen bonds or salt bridges. In contrast, most of the side chains at the intertrimeric interfaces are not required individually for capsid assembly or stability against dissociation. Some of these residues participate in only a limited number of intertrimer van der Waals interactions; others are involved additionally in one or two hydrogen bonds and/or charge–charge interactions that, to different extents, were exposed to solvent on the virus capsid. The individual contribution of interfacial residues to intersubunit association energies have been theoretically predicted for the MVMi capsid and for other viruses as well, and the results are available from the Virus Particle Explorer (VIPER; available at http://mmtsb.scripps.edu/viper/viper.html) (53). A comparison with our experimental results revealed that four of the seven side chains whose truncation prevented assembly corresponded to residues predicted to be energetically important (association energy −2.0 to −4.6 kcal/mol). In contrast, all but three of the 21 tested side chains that were individually dispensable for assembly and stability corresponded to residues predicted to be less energetically important (association energy −0.3 to −1.7 kcal/mol). Only the very few side chains involved in intersubunit noncovalent interactions that may be considered to be energetically stronger were found to be critical individually for capsid assembly and stability. The noncritical interfacial residues tested were found scattered at random at the trimer boundaries, as expected. In striking contrast, the 21 (7×3) residues per trimer that were found to be critical for capsid assembly delineated a buried, thin equatorial belt of regularly spaced individual residues or small clusters (Fig. 3). This remarkable regularity is not just a symmetry effect because it is preserved even within each individual VP2 molecule.

The direct involvement in assembly and stability of only a few residues at the intertrimer interfaces does not indicate that the remaining residues at these defined capsid regions are functionally irrelevant and tolerant to mutation. In fact, the interfacial residues closer to the pores at the capsid five-fold axes (Fig. 5) are involved in a conformational rearrangement of the capsid that includes, but is not limited to, externalization of the N-terminal segment of VP2 through those pores. Recently, a normally externalized sequence within the VP2 N terminus has been shown to be required for nuclear egress of mature MVM particles and viral infectivity (B. Maroto, N. Valle, R. Saffrich, and J.M.A., unpublished data). Mutation of the residues surrounding the base of the pores at the five-fold axes prevented the conformational rearrangement of the capsid and impaired externalization of the VP2 N terminus. Thus, their critical effect on infectivity may be related to reduced cell-to-cell spreading because of the difficulty of progeny viruses to be exported from the cell nucleus. Moreover, truncation of some of the interfacial side chains that were found not to be involved in assembly, stability against dissociation, or the detected conformational change also impaired infectivity to some extent. These results add to our previous observations and those of other researchers (22–27) on physical overlaps between the residues and substructures that are responsible for the many functions of a viral capsid. Such overlapping may have arisen as an adaptive solution to provide relatively simple homooligomeric protein capsids with several complex functions, but it may impose, as a consequence, important structural and functional constraints to virus evolution.

We thank J. Rodríguez, A.L. Carrascosa, A. Alejo, A. López-Bueno, and C. Epifanio for technical advice; C.R. Parrish for MAb B7; and P. Tattersall for clone pMM984. This work was supported by independent grants from Ministerio de Ciencia y Tecnología and the Comunidad Autónoma de Madrid (to the laboratories of M.G.M. and J.M.A.) and an institutional grant from the Fundación Ramón Areces.

1. Bogan, A. A. & Thorn, K. S. (1998) *J. Mol. Biol.* **280,** 1–9.
2. Del Álamo, M., Neira, J. L. & Mateu, M. G. (2003) *J. Biol. Chem.* **278,** 27923–27929.
3. Milla, M. E., Brown, B. M. & Sauer, R. T. (1994) *Nat. Struct. Biol.* **1,** 518–523.
4. Mateu, M. G. & Fersht, A. R. (1998) *EMBO J.* **17,** 2748–2758.
5. Liljas, L. (1986) *Prog. Biophys. Mol. Biol.* **48,** 1–36.
6. Rossmann, M. G. & Johnson, J. E. (1999) *Annu. Rev. Biochem.* **58,** 533–573.
7. Filman, D. J., Syed, R., Chow, M., Macadam, A. J., Minor, P. D. & Hogle, J. M. (1989) *EMBO J.* **8,** 1567–1579.
8. Zhou, S. & Standring, D. N. (1992) *J. Virol.* **66,** 5393–5398.
9. Stonehouse, N. J. & Stockley, P. G. (1993) *FEBS Lett.* **334,** 355–359.
10. Foguel, D., Teschke, C. M., Prevelige, P. E. & Silva, J. L. (1995) *Biochemistry* **34,** 1120–1126.
11. Culver, J. N., Dawson, W. O., Plonk, K. & Stubbs, G. (1995) *Virology* **206,** 724–730.
12. Stonehouse, N. J., Valegard, K., Golmohammadi, R., van der Worm, S., Walton, C., Stockley, P. G. & Liljas, L. (1996) *J. Mol. Biol.* **256,** 330–339.
13. Wien, M. W., Curry, S., Filman, D. J. & Hogle, J. M. (1997) *Nat. Struct. Biol.* **4,** 666–674.
14. Bendahmane, M., Fitchen, J. H., Zhang, G. & Beachy, R. N. (1997) *J. Virol.* **71,** 7942–7950.
15. Parker, J. S. L. & Parrish, C. R. (1997) *J. Virol.* **71,** 9214–9222.
16. Wang, W., Lee, W. M., Mosser, A. G. & Rueckert, R. R. (1998) *J. Virol.* **72,** 1210–1218.
17. Sastri, M., Reddy, D. S., Krishna, S. S., Murthy, M. R. N. & Savithri, H. S. (1999) *J. Mol. Biol.* **289,** 905–918.
18. Ellard, F. M., Drew, J., Blakemore, W. E., Stuart, D. I. & King, A. M. (1999) *J. Gen. Virol.* **80,** 1911–1918.
19. Limn, C.-K., Staeuber, N., Monastyrskaya, K., Gouet, P. & Roy, P. (2000) *J. Virol.* **74,** 8658–8669.
20. Wu, P., Xiao, W., Conlon, T., Hughes, J., Agbandje-McKenna, M., Ferkol, T., Flotte, T & Mucyczka, N. (2000) *J. Virol.* **74,** 8635–8647.
21. Bertolotti-Ciarlet, A., White, L. J., Chen, R., Prasad, B. V. V. & Estes, M. K. (2002) *J. Virol.* **76,** 4044–4055.
22. Mateo, R., Díaz, A., Baranowski, E. & Mateu, M. G. (2003) *J. Biol. Chem.* **278,** 41019–41027.
23. Rossmann, M. G., Greve, J. M., Kolatkar, P. R., Olson, N. H., Smith, T. J., McKinlay, M. A. & Rueckert, R. R. (1997) in *Structural Biology of Viruses*, eds. Chiu, W., Garcea, R. & Burnette, R. (Oxford Univ. Press, Oxford), pp.105–133.
24. Johnson, J. E. (1996) *Proc. Natl. Acad. Sci. USA* **93,** 27–33.
25. Chow, M., Basavappa, R. & Hogle, J. M. (1997) in *Structural Biology of Viruses*, eds. Chiu, W., Garcea, R. & Burnette, R. (Oxford Univ. Press, Oxford), pp. 157–186.
26. Reddy, V. S., Giesing, H. A., Morton, R. T., Kumar, A., Post, C. B., Brooks III, C. L. & Johnson, J. E. (1998) *Biophys. J.* **74,** 546–558.
27. Mateu, M. G. (1995) *Virus Res.* **38,** 1–24.
28. Rossmann, M. G. (1990) in *Use of X-Ray Crystallography in the Design of Antiviral Agents*, eds. Laver, W. G. & Air, G. M. (Academic, New York), pp. 115–137.
29. Wien, M. W., Chow, M. & Hogle, J. M. (1996) *Structure (London)* **4,** 763–767.
30. Diana, G. D., McKinlay, M. A. & Treasurywala, A. (1997) In *Structural Biology of Viruses*, eds. Chiu, W., Garcea, R. & Burnette, R. (Oxford Univ. Press, Oxford), pp. 432–450 .
31. Belnap, D. M., Filman, D. J., Trus, B. L., Cheng, N., Booy, F. P., Conway, J. F., Curry, S., Hiremath, C. N., Tsang, S. K., Steven, A. C. & Hogle, J. M. (2000) *J. Virol.* **74,** 1342–1354.
32. Tsao, J., Chapman, M. S., Agbandje, M., Keller, W., Smith, K., Wu, H., Luo, M., Smith, T. J., Rossmann, M. G., Compans, R. W. & Parrish, C. R. (1991) *Science* **251,** 1456–1464.
33. Wu, H. & Rossmann, M. G. (1993) *J. Mol. Biol.* **233,** 231–244.
34. Agbandje, M., McKenna, R., Rossmann, M. G., Strassheim, M. L. & Parrish, C. R. (1993) *Proteins* **16,** 155–171.
35. Llamas-Saiz, A. L., Agbandje-McKenna, M., Wikoff, W. R., Bratton, J., Tattersall, P. & Rossmann, M. G. (1997) *Acta Crystallogr.* **D53,** 93–102.
36. Agbandje-McKenna, M., Llamas-Saiz, A. L., Wang, F., Tattersall, P. & Rossmann, M. G. (1998) *Structure (London)* **6,** 1369–1381.
37. Simpson, A. A., Hebert, B., Sullivan, G. M., Parrish, C. R., Zadori, Z., Tijssen, P. & Rossmann, M. G. (2002) *J. Mol. Biol.* **315,** 1189–1198.
38. Hernando, E., Llamas-Saiz, A. L., Foces-Foces, C., McKenna, R., Portman, I., Agbandje-McKenna, M. & Almendral, J. M. (2000) *Virology* **267,** 299–309.
39. Cotmore, S. F. & Tattersall, P. (1987) *Adv. Virus Res.* **33,** 91–174.
40. Tattersall, P., Shatkin, A. J. & Ward, D. C. (1977) *J. Mol. Biol.* **111,** 375–394.
41. Cotmore, S. F., D-Abramo, Jr., A. M., Ticknor, C. M. & Tattersall, P. (1999) *Virology* **254,** 169–181.
42. Yuan, W. & Parrish, C. R. (2001) *Virology* **279,** 546–557.
43. Chapman, M. S. & Rossmann, M. G. (1993) *Virology* **194,** 491–508.
44. Lombardo, E., Ramírez, J. C., Agbandje-McKenna, M. & Almendral, J. M. (2000) *J. Virol.* **74,** 3804–3814.
45. Lombardo, E., Ramírez, J. C., García, J. & Almendral, J. M. (2002) *J. Virol.* **76,** 7049–7059.
46. Ramírez, J. C., Santarén, J. F. & Almendral, J. M. (1995) *Virology* **206,** 57–68.
47. Carreira, A., Menéndez, M., Reguera, J., Almendral, J. M. & Mateu, M. G. (2004) *J. Biol. Chem.* **279,** 6517–6525.
48. Gardiner, E. M. & Tattersall, P. (1988) *J. Virol.* **62,** 2605–2613.
49. Sayle, R. A. & Milner-White, E. J. (1995) *Trends Biochem. Sci.* **20,** 374–376.
50. Vriend, G. (1990) *J. Mol. Graphics.* **8,** 52–56.
51. Zlotnick, A. (1994) *J. Mol. Biol.* **241,** 59–67.
52. López-Bueno, A., Mateu, M. G. & Almendral, J. M. (2003) *J. Virol.* **77,** 2701–2708.
53. Reddy, V. S., Natarajan, P., Okerberg, B., Li, K., Damodaran, K. V., Morton, R. T., Brooks III, C. L. & Johnson, J. E. (2001) *J. Virol.* **75,** 11943–11947.